Imaging T-cell receptor activation reveals accumulation of tyrosine-phosphorylated CD3ζ in the endosomal compartment

Ivan A. Yudushkin and Ronald D. Vale[1]

Department of Cellular and Molecular Pharmacology, University of California, San Francisco, CA 94158

Contributed by Ronald D. Vale, November 9, 2010 (sent for review September 6, 2010)

Phosphorylation of the T-cell receptor complex (TcR/CD3) mediates the survival and antigen-induced activation of T cells. TcR/CD3 phosphorylation is usually monitored using phospho-specific antibodies, which precludes dynamic measurements. Here, we have developed genetically encoded, live-cell reporters that enable simultaneous monitoring of the phosphorylation state and intracellular trafficking of CD3ζ, the major signal-transducing subunit of the TcR/CD3. We show that these reporters provide accurate readouts of TcR/CD3 phosphorylation and are sensitive to the local balance of kinase and phosphatase activities acting upon TcR/CD3. Using these reporters, we demonstrate that, in addition to the expected activation-dependent phosphorylation at the plasma membrane, tyrosine-phosphorylated CD3ζ accumulates on endosomal vesicles distinct from lysosomes. These results suggest that an intracellular pool of phosphorylated CD3ζ may help to sustain TcR/CD3 signaling after the receptor internalization.

Förster's resonant energy transfer | receptor trafficking | Lck kinase

The interaction between the T-cell receptor (TcR) and peptide:MHC complex on antigen-presenting cells mediates physiological responses of T cells. To transmit the signal through the plasma membrane, the TcR uses a multimeric CD3 complex whose subunits (γ-, δ-, ε-, and ζ chains) contain one or more *immunoreceptor tyrosine-based activation motifs* (ITAMs). Upon TcR ligation, the two tyrosine residues in the ITAMs (**Y**xx[L/I]x_{6-9}**Y**xx[L/I]) are phosphorylated by the Src family kinases Lck and Fyn. The dually phosphorylated ITAMs serve as a binding platform for molecules involved in TcR/CD3-proximal signaling, most importantly the tyrosine kinase ZAP-70, which phosphorylates downstream targets (1). Activation-dependent tyrosine phosphorylation of the ITAM-containing chains of the CD3 complex leads to TcR/CD3 internalization and, eventually, degradation in lysosomes (2, 3).

Recent studies using high-resolution imaging have demonstrated that signaling via TcR/CD3 displays complex spatial organization. TcR/CD3 molecules are preclustered at the plasma membrane and, upon ligation, nucleate downstream signaling components seconds after T-cell activation (4, 5). TcR/CD3 is constitutively internalized and recycled to the plasma membrane in naïve and activated T cells (reviewed in ref. 6), but the function of this turnover as well as the phosphorylation state of internalized receptor remain unknown.

Currently, phosphorylation of TcR/CD3 in cells and in vitro is monitored using phospho-specific antibodies, and there are no methods that enable dynamic monitoring of the spatial organization of CD3 phosphorylation in live cells. Here, we have constructed genetically encoded fluorescent reporters compatible with imaging of live and fixed cells and demonstrate that they accurately monitor the dynamics and intracellular organization of CD3ζ phosphorylation in Jurkat T cells. Using the reporters, we observed that in addition to the expected activation-dependent phosphorylation at the plasma membrane, tyrosine-phosphorylated CD3ζ accumulated in the perinuclear endosomal vesicles. Our results demonstrate that endosomal CD3ζ remains signaling-competent and suggest the possibility that internalized CD3ζ pool may help to sustain long-term signaling in T cells.

Results

Design and Characterization of the CD3ζ Phosphorylation Reporters. To generate a Förster's resonant energy transfer (FRET)-based monomolecular reporter for phosphorylation of the key CD3 signal-transducing subunit ζ, we fused the C terminus of CD3ζ to a pair of green and red fluorescent proteins, eGFP and mCherry, linked by a flexible spacer and followed by the tandem SH2 domains of human ZAP-70 (residues 1–259; $tSH2^{ZAP\text{-}70}$). We reasoned that intramolecular binding of the SH2 domains to tyrosine-phosphorylated ITAMs of CD3ζ (7) would result in conformational rearrangement of the adjacent fluorescent proteins and change in the FRET efficiency between the donor (eGFP) and acceptor (mCherry) fluorophores (Fig. 1*A* and *SI Text*). We found that the length of the spacer between the eGFP and mCherry was important for optimizing the dynamic range of the reporter. The initial probe with a shorter 12-aa-long spacer displayed high FRET but failed to report changes in CD3ζ phosphorylation, whereas the longer 17-aa-long spacer yielded the desired reporter, in which FRET efficiency changed in response to signaling cues, herein referred to as the CD3zeta ITAM phosphorylation (ZIP) reporter.

We first tested whether the reporter could be phosphorylated in cells in a manner similar to the endogenous CD3ζ. Inhibition of phosphotyrosine phosphatases by sodium pervanadate in Jurkat cells stably expressing the ZIP reporter enhanced phosphorylation of both the endogenous CD3ζ and the ZIP reporter (Fig. 1*B* and Fig. S1*A*). The basal and pervanadate-induced phosphorylation decreased upon preincubation with the Src-family tyrosine kinase inhibitor PP2 (Fig. 1*B*). Mutation of the six tyrosine residues to phenylalanine in all three ITAMs precluded tyrosine phosphorylation of the ZIP^{YF} reporter, but not of endogenous CD3ζ (Fig. 1*B*). Collectively, these biochemical results indicate that phosphorylation of the reporter parallels that of the endogenous CD3ζ.

Next, we tested whether phosphorylation of the reporter could be observed in cells using time-correlated single-photon counting fluorescence lifetime imaging microscopy (TCSPC-FLIM) to monitor FRET. For Jurkat cells adhered to glass coverslips precoated with the stimulatory anti-CD3 mAb HIT3a, a high (25–40%) FRET efficiency was observed (Fig. 1*C*). Acceptor photobleaching resulted in a significant increase of mean eGFP lifetime from ≈1.4–1.6 to 1.9–2.0 ns, confirming that the lower eGFP lifetime in cells is due to FRET. We could also detect

Author contributions: I.A.Y. and R.D.V. designed research; I.A.Y. performed research; I.A.Y. analyzed data; and I.A.Y. and R.D.V. wrote the paper.

The authors declare no conflict of interest.

Freely available online through the PNAS open access option.

Data deposition: The DNA constructs reported in this paper have been deposited in the AddGene Repository, www.addgene.org/Ron_Vale (accession nos. 27134–27137).

[1]To whom correspondence should be addressed. E-mail: vale@cmp.ucsf.edu.

This article contains supporting information online at www.pnas.org/lookup/suppl/doi:10.1073/pnas.1016388108/-/DCSupplemental.

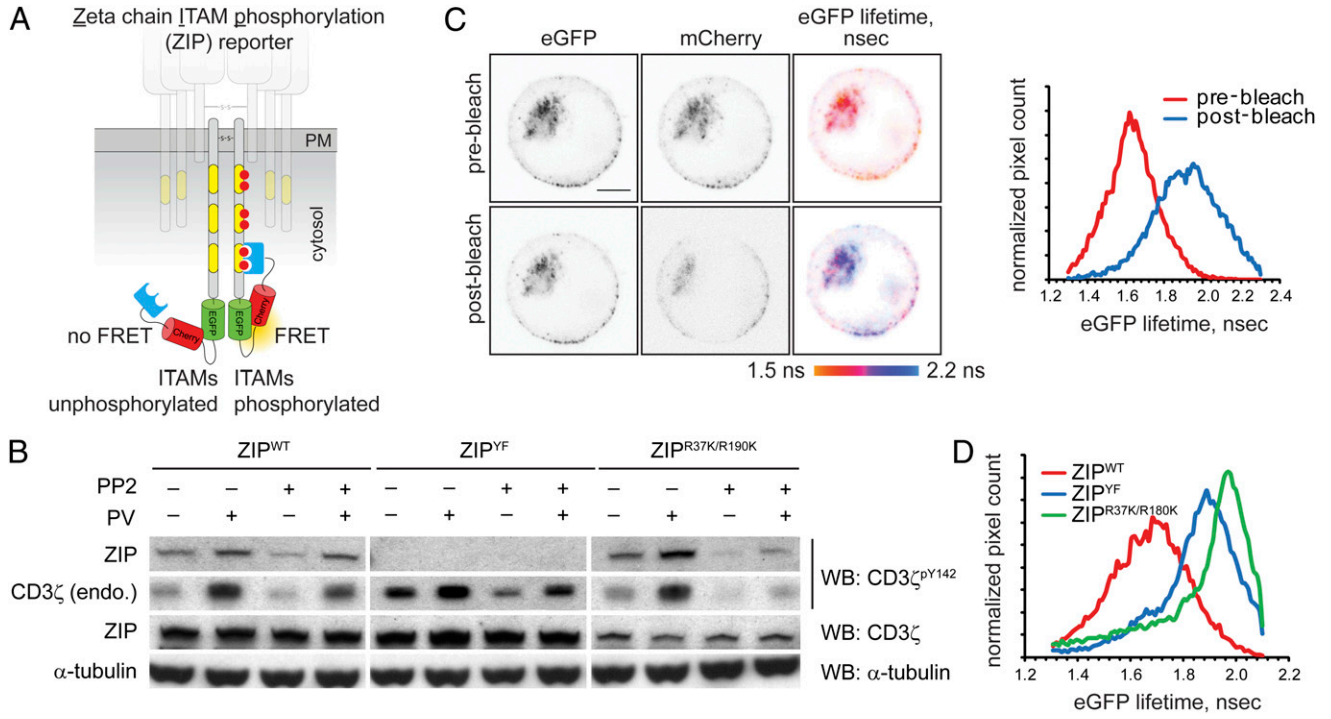

Fig. 1. Design and characterization of the ZIP reporter. (*A*) Intramolecular binding of the SH2 domains to tyrosine-phosphorylated ITAMs within the ZIP reporter results in FRET between GFP and mCherry. (*B*) Jurkat cells stably expressing the ZIP^{WT} reporter or the ZIP^{YF} or ZIP$^{R37K/R190K}$ mutants were preincubated with the generic Src family kinase inhibitor PP2 (2 μM) or the vehicle for 30 min and then stimulated for 5 min with 100 μM sodium pervanadate (PV). Cell lysates were analyzed by Western blotting (WB) using mAb against CD3ζ^{pY142}, pan-CD3ζ, and α-tubulin. Full-length blots are presented in Fig. S1*A*. (*C*) Jurkat cells stably expressing the ZIP^{WT} reporter were adhered onto glass coverslips precoated with 20 μg/mL anti-CD3 mAb HIT3a, and eGFP lifetime before and after photobleaching of the acceptor (mCherry) was monitored using TCSPC-FLIM. Shown are the confocal images in the eGFP and mCherry channels and the corresponding pseudocolored eGFP fluorescence lifetime images scaled between 1.5 and 2.2 ns. (Scale bar, 2 μm.) *Right:* Corresponding cumulative histograms of the eGFP lifetime before and after acceptor photobleaching. (*D*) Cumulative histograms of eGFP lifetime in Jurkat cells stably expressing the ZIP^{WT} reporter or ZIP^{YF} or ZIP$^{R37K/R190K}$ mutants, adhered onto glass coverslips precoated with 20 μg/mL HIT3 mAb for 10 min.

sensitized emission from the acceptor, which rapidly increased upon receptor ligation by the anti-CD3 antibody. Furthermore, pixels displaying high FRET signal in the ZIP reporter-expressing cells colocalized well with immunofluorescent staining by a mAb specific for CD3ζ^{pY142} (Fig. S1*B*). Accessibility of this epitope for the mAb in fixed cells suggests that the tandem SH2 domains of the ZIP reporter likely bind phosphotyrosine residues in ITAMs 1 or 2, in line with previous findings (8). Together, these data demonstrate that the observed FRET signal corresponds to phosphorylation of tyrosine residues within the ITAMs of the reporter.

To examine the specificity of the observed FRET signal and test whether it resulted from intramolecular binding of tSH2$^{ZAP\text{-}70}$ to phosphorylated ITAMs, we imaged FRET efficiency in cells expressing the ZIP^{YF} mutant of the reporter. Consistent with biochemical data (Fig. 1*B*), the ITAMs in the ZIP^{YF} mutant could not be phosphorylated and thus displayed a significantly lower (<10%) FRET efficiency (Fig. 1*D*). We found, however, that acceptor photobleaching in the ZIP^{YF} mutant resulted in further increase of eGFP lifetime from ≈1.9 to 2.2 ns, typical for unquenched eGFP (Fig. S1*C*), indicating that low basal FRET is observed in the absence of ITAM phosphorylation. Introduction of the double point mutation R37K/R190K, which disrupts binding of the SH2 domains to phosphotyrosine residues (9), resulted in the eGFP lifetime of ≈2.0 ns, similar to that of ZIP^{YF} (Fig. 1*D*), suggesting that the low basal FRET signal is likely to result from juxtaposition of fluorescent proteins in the reporter homodimer.

Endogenous ZAP-70 could compete with the tSH2$^{ZAP\text{-}70}$ of the reporter for binding to phosphorylated ITAMs. Indeed, we found that in the ZAP-70–deficient line P116, the activation-induced FRET was higher than in the wild-type (E6.1) Jurkat cells (Fig. S1*D*). Thus, low basal FRET within the reporter homodimer (Fig. S1*E*) as well as competition with endogenous ZAP-70 somewhat limit the dynamic range of the FRET signal in the ZIP reporter. Nevertheless, the above results indicate that the ZIP reporter mimics the behavior of endogenous CD3ζ and demonstrate that its phosphorylation state can be faithfully monitored in cells using FLIM.

To better characterize the rapid dynamics of CD3 phosphorylation at the plasma membrane and probe phosphorylation state of endogenous CD3, we developed an alternative reporter consisting of tSH2$^{ZAP\text{-}70}$ fused with the red fluorescent protein mCherry (mCherry-tSH2$^{ZAP\text{-}70}$; Fig. 2*A*). We reasoned that in unstimulated cells the reporter, like ZAP-70, would reside in the cytosol but will associate with tyrosine-phosphorylated ITAMs of the CD3 subunits upon activation. This translocation from the cytosol to the plasma membrane can be readily detected by confocal or total internal reflection fluorescence (TIRF) microscopy. Indeed, in unstimulated cells mCherry-tSH2$^{ZAP\text{-}70}$ was mostly cytosolic but translocated to the plasma membrane upon activation by anti-CD3 antibody or in response to pervanadate (Fig. 2*B* and Movie S1).

To test whether membrane translocation of the reporter was indeed caused by its binding to tyrosine-phosphorylated ITAMs of the CD3 complex, we monitored FRET between mCherry-tSH2$^{ZAP\text{-}70}$ and eGFP-tagged CD3ζ subunit cotransfected in the same cell (Fig. 2*C*). In unstimulated cells, little FRET was observed at the plasma membrane. Cell activation by pervanadate resulted in increased FRET, demonstrating that translocation of mCherry-tSH2$^{ZAP\text{-}70}$ reporter to the plasma membrane is caused by its interaction with tyrosine-phosphorylated ITAMs. Together,

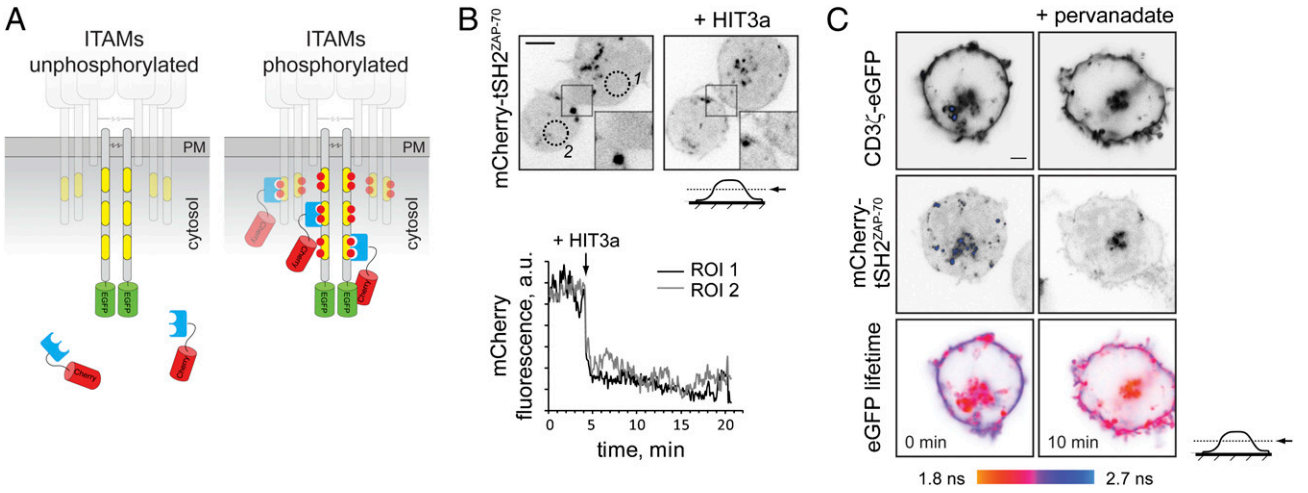

Fig. 2. Design and characterization of the bimolecular translocation reporter. (*A*) Binding of the reporter to the phosphorylated ITAMs is detected by its translocation to the membrane and/or FRET between the eGFP-tagged CD3 subunit and mCherry of the reporter. (*B*) Jurkat cells expressing mCherry-tSH2^{ZAP-70} were allowed to adhere onto a glass-bottom dish coated with poly-D-lysine. Shown is the localization of the reporter before (*Left*) and ≈10 min after (*Right*) addition of 10 μg/mL mAb HIT3a (*Upper*). The chart demonstrates activation-dependent depletion of the reporter from cytosol and its translocation to the plasma membrane upon addition of HIT3a in both regions of interest (ROI). Full time-lapse sequence is presented in Movie S1. (Scale bar, 5 μm.) (*C*) Jurkat cells transiently coexpressing CD3ζ-eGFP and mCherry-tSH2^{ZAP-70} reporter were allowed to adhere onto a glass-bottom dish coated with poly-D-lysine, and eGFP fluorescence lifetime before and 10 min after addition of 1 mM sodium pervanadate was monitored using TCSPC-FLIM. The images were acquired at the midcell level, so that intracellular vesicles are clearly seen. Shown are confocal images of CD3ζ-eGFP, mCherry-tSH2^{ZAP-70}, and the corresponding pseudocolored eGFP lifetime images, scaled between 1.8 and 2.7 ns. A different scale in the eGFP lifetime images is due to lower FRET efficiency observed for bimolecular interaction between CD3ζ-eGFP and mCherry-tSH2^{ZAP70} than the intramolecular interaction for the ZIP^{WT} reporter. (Scale bar, 2 μm.)

these results demonstrate that mCherry-tSH2^{ZAP-70} could be used for monitoring the intracellular localization and rapid phosphorylation dynamics of the ITAM-containing subunits, even those expressed at the endogenous levels.

CD3ζ Phosphorylation Is Controlled by a Dynamic Reaction Cycle. To test whether the dynamic range of the FRET signal is sufficient to monitor changes in phosphorylation state of the ZIP reporter, we incubated the wild-type (E6.1) Jurkat cells stably expressing the ZIP reporter on glass coverslips precoated with the stimulatory anti-CD3 mAb (HIT3a) or the corresponding isotype control and determined eGFP lifetime in fixed cells using FLIM (Fig. 3 *A* and *B*). As expected, TcR ligation by an anti-CD3, but not isotype control antibody, resulted in ITAM phosphorylation and decreased eGFP lifetime, indicative of FRET. In line with biochemical results, only low basal FRET signal was

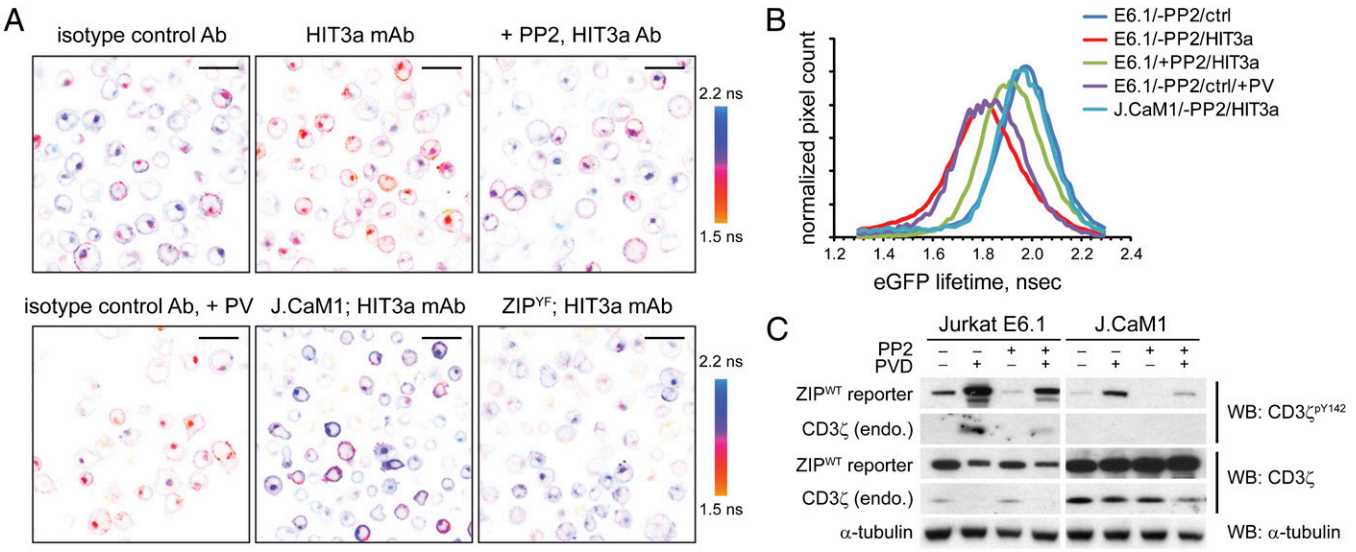

Fig. 3. CD3ζ phosphorylation is controlled by a dynamic reaction cycle. (*A*) Wild-type Jurkat E6.1 or Lck-deficient J.CaM1 (*Lower Center*) cells stably expressing the ZIP^{WT} reporter or the ZIP^{YF} mutant (*Lower Right*) were preincubated with 2 μM PP2 or the vehicle (DMSO) for 30 min and then adhered onto a glass coverslip precoated with 20 μg/mL mAb HIT3a or the respective isotype control antibody for 10 min, fixed, and eGFP lifeime monitored using TCSPC-FLIM. Shown are pseudocolored eGFP lifetime images of typical regions of interest (ROIs), scaled between 1.5 and 2.2 ns. (Scale bars, 20 μm.) (*B*) Cumulative histograms of the eGFP lifetime averaged over 3 to 4 ROIs of cells stimulated as described for Fig. 2*A*. (*C*) Wild-type Jurkat E6.1 or Lck-deficient J.CaM1 cells stably expressing the ZIP^{WT} reporter were preincubated with 2 μM PP2 or the vehicle (DMSO) for 30 min and then stimulated for 5 min with 100 μM sodium pervanadate. The lysates were analyzed by Western blotting using mAbs against CD3ζ^{pY142}, pan-CD3ζ, and α-tubulin. Full-length blots are presented in Fig. S2*A*.

detected in cells expressing ZIP^{YF} mutant on the anti-CD3–coated surface.

We next examined whether the phosphorylation state of the ZIP reporter is altered by perturbations to tyrosine kinases and phosphotyrosine phosphatases. Lck and Fyn are the primary tyrosine kinases that phosphorylate ITAMs of the CD3 complex in T cells (10, 11). Consistent with previous results (10), we found reduced phosphorylation and degradation of ZIP^{WT} in the Lck-deficient cell line J.CaM1, suggesting that the reporter is a substrate for tyrosine phosphorylation by Lck (Fig. 3*C*). Conversely, inhibition of phosphotyrosine phosphatases by pervanadate in Jurkat E6.1 cells resulted in rapid increase of the reporter phosphorylation (Fig. 3*C*). Similar results were observed using FLIM: in the Lck-deficient J.CaM1 cells the reporter displayed higher lifetime (Fig. 3 *A* and *B*), although a small fraction of cells demonstrated higher FRET signal at the plasma membrane. As expected, lower fluorescence lifetime was observed after a short (5 min) treatment of the wild-type Jurkat cells with pervanadate (Fig. 3*A*). These results indicate that the phosphorylation of the ITAM motifs in the reporter is under tonic control of phosphatases.

Tandem SH2 domains of ZAP-70 were reported to have a dominant-negative effect on downstream signaling (12), suggesting that irreversible intramolecular binding of the tSH2$^{ZAP\text{-}70}$ in the reporter could protect phosphorylated ITAMs from the action of phosphotyrosine phosphatases. Inhibition of the Src family kinases by PP2, however, resulted in the rapid (<5 min) decrease of FRET, demonstrating that intramolecular binding of tSH2$^{ZAP\text{-}70}$ to tyrosine-phosphorylated ITAMs in the reporter is readily reversible (Fig. S2*B*). Furthermore, preincubation with PP2 diminished anti-CD3 antibody-induced reporter phosphorylation in Jurkat cells (Fig. 3 *A* and *B*). These results further demonstrate that the reporter mimics the behavior of endogenous CD3ζ and that its net phosphorylation is a product of the dynamic reaction cycle consisting of tyrosine kinases and phosphotyrosine phosphatases.

Intracellular Organization of CD3ζ Phosphorylation. Previous studies demonstrated activation-dependent formation of TcR/CD3-containing microclusters enriched with signaling molecules at the plasma membrane. In line with these reports (13, 14), we observed that in cells activated by anti-CD3–functionalized lipid bilayer, mCherry-tSH2$^{ZAP\text{-}70}$ translocated to the centripetally moving microclusters at the plasma membrane, eventually resulting in the formation of a central supramolecular activation cluster-like structure (Fig. S3*A* and Movie S2). Similar membrane-proximal clusters that displayed a high FRET signal were observed in ZIP^{WT}-expressing cells placed on a glass-bottom dish precoated with anti-CD3 antibody. These membrane clusters colocalized with immunostaining against tyrosine-phosphorylated CD3ζ and excluded membrane phosphotyrosine phosphatase CD45 (Fig. S3*B*). Our findings are in agreement with earlier studies demonstrating that CD3 phosphorylation and TcR-proximal signaling are initiated and sustained in TcR/CD3 microclusters at the plasma membrane (5, 13, 14).

TcR ligation by a surface-bound anti-CD3 antibody or phosphatase inhibition by pervanadate resulted in increased ZIP reporter phosphorylation at the plasma membrane, followed by formation of membrane-proximal endosomal vesicles containing the reporter (Fig. S3*C*). Cells displayed a prominent activation-dependent FRET signal and increased CD3ζ^{pY142} antibody staining at the perinuclear compartment (Figs. 2*C* and 3*A* and Fig. S1*B*), indicating that tyrosine-phosphorylated CD3ζ accumulated in these intracellular vesicles.

Unexpectedly, we observed that a subpopulation of unstimulated cells also displayed increased phosphorylation of the ZIP reporter in what appeared to be an intracellular vesicular compartment, whereas low FRET was detected at the plasma membrane (Fig. 3*A*). Similar results were observed using the translocation reporter, whereby mCherry-tSH2$^{ZAP\text{-}70}$ accumulated on the CD3ζ-eGFP–containing intracellular vesicles in a subset of nonstimulated cells (Fig. 2*C*). Furthermore, accumulation of the tyrosine-phosphorylated material was observed for endogenous CD3ζ, as revealed by direct immunostaining with specific mAb against CD3ζ^{pY142} (Fig. S4*A*). Preincubation with PP2 decreased FRET in the intracellular vesicles (Fig. 3*A*), suggesting that in unstimulated cells this vesicular compartment may represent a site for accumulation of basally phosphorylated CD3ζ.

Accumulation of CD3ζ in the perinuclear vesicles was previously observed for endogenous and GFP-tagged CD3ζ in several Jurkat clones, naïve T cells, and T-cell hybridomas (8, 15–18) and is consistent with constitutive internalization and recycling of the TcR/CD3 described in various primary cells and cell lines. Indeed, time-lapse microscopy shows that the ZIP reporter-containing vesicles actively move within the cytoplasm and exchange with the plasma membrane (Movie S3). Blocking of the clathrin-mediated endocytosis by a membrane-permeable dynamin inhibitor Dynasore dramatically reduced fluorescence recovery after photobleaching of the reporter in the perinuclear vesicles, indicating that they accumulated material internalized from the plasma membrane (Fig. S4*B*).

Next, we investigated the nature of the perinuclear vesicular compartment. A subpopulation of internalized CD3ζ-eGFP colocalized with markers of early and recycling endosomes Rab5 and Rab11 (Fig. 4*A*), which is particularly evident in time-lapse movies (Movies S4 and S5). To further investigate the identity of the CD3ζ-containing vesicles, we examined the intracellular localization of the ZIP reporter using immunofluorescent staining for markers of various endocytic compartments. Internalized reporter did not colocalize with *cis*-Golgi marker GM130 but partially colocalized with markers for early (EEA1) and recycling endosomes (Rab11), *trans*-Golgi compartment (TGN46), and the lysosomal marker LAMP1 (Fig. S4*C*), demonstrating that internalized CD3ζ is distributed across the compartments of the endosomal recycling network. Endosomal accumulation was not due to abnormal intracellular trafficking of the ZIP reporter, because myc-tagged CD3ζ displayed similar localization at the plasma membrane and on endosomes (Fig. S4*D*).

Prior studies (2, 3, 18, 19) indicated that internalized TcR/CD3 in stimulated cells is targeted for degradation; therefore, we examined colocalization of the reporter or CD3ζ-eGFP with lysosomes using immunofluorescent staining with the lysosomal markers LAMP1 or LysoTracker Red. In unstimulated cells, only a fraction of internalized CD3ζ colocalized with fluorescent lysosomes (Fig. S4*E*), similar to previously published data (17). Furthermore, internalized tyrosine-phosphorylated ZIP^{WT} reporter displaying high FRET signal was present in vesicles clearly distinct from lysosomes (Fig. 4*B*). In agreement with a previous report (18), cell stimulation by pervanadate depleted CD3ζ-eGFP from the plasma membrane and increased the number of endocytic vesicles containing CD3ζ-eGFP (Movie S6), although a significant fraction of internalized CD3ζ was concentrated in vesicles clearly distinct from lysosomes. This demonstrates that although some of the activated CD3ζ is targeted for lysosomes, a subpopulation of internalized, tyrosine-phosphorylated CD3ζ is retained in the endosomal compartment.

Next, we examined whether tyrosine-phosphorylated reporter at the plasma membrane exchanged with the internalized CD3ζ pool. TcR ligation results in formation of plasma membrane-proximal endosomes, containing tyrosine-phosphorylated reporter (Fig. S3*C* and Movie S7). Acceptor (mCherry) photobleaching of the reporter in the endosomal compartment resulted in FRET failure, observed as increased eGFP lifetime (Fig. 4*C*). However, both mCherry fluorescence and FRET signal in the intracellular vesicles gradually restored with kinetics similar to the reporter internalization rate (Fig. S4 *B* and *F*), indicating that tyrosine-phosphorylated CD3ζ is transported from the plasma

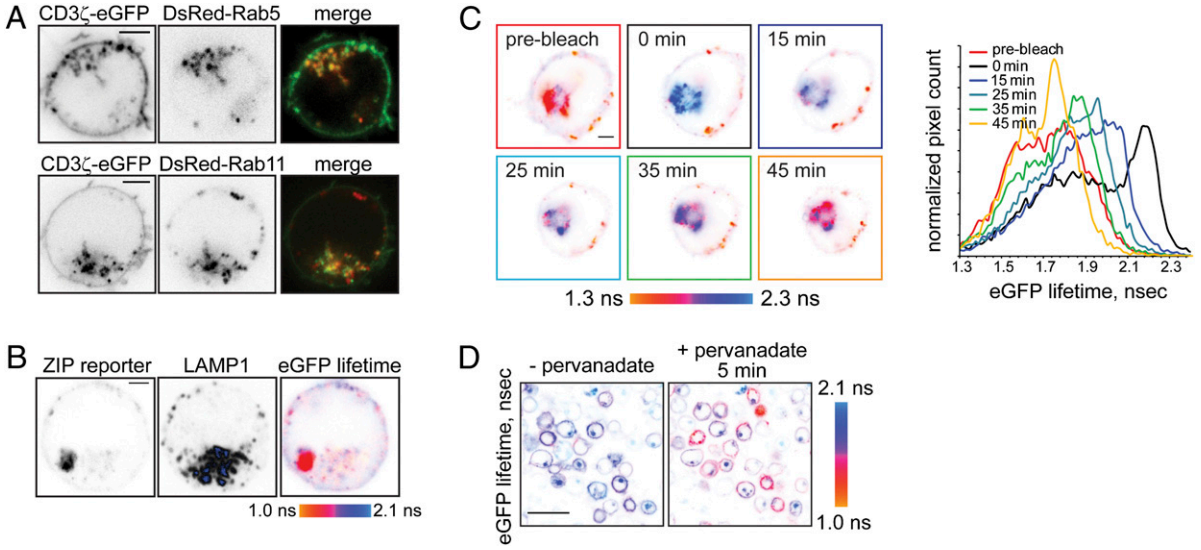

Fig. 4. Lck locally phosphorylates CD3ζ at the plasma membrane and on endosomes. (*A*) Jurkat E6.1 cells, transiently coexpressing CD3ζ-eGFP and either DsRed-tagged Rab5 (*Upper*) or Rab11 (*Lower*), were adhered onto a poly-D-lysine–coated glass-bottom dish. Shown are the confocal images in the eGFP or DsRed channels and the confocal overlay at the midcell level, so that intracellular vesicles are clearly seen. Time-lapse sequences are presented in Movies S4 and S5. (Scale bars, 2 μm.) (*B*) ZIP^{WT} reporter-expressing Jurkat cell was fixed and immunostained using mouse LAMP1 antibody and secondary goat anti-mouse Alexa647-conjugated Ab. Shown are the confocal images of the reporter in the eGFP channel and antibody in the far-red channel, as well as the corresponding eGFP lifetime image, scaled between 1.0 and 2.1 ns. Internalized tyrosine-phosphorylated reporter is present in intracellular vesicles distinct from lysosomes. Low-background signal colocalizing with the LAMP1 staining likely indicates degradation of the reporter in the lysosomes. (Scale bar, 2 μm.) (*C*) Jurkat cell transiently expressing the ZIP^{WT} reporter was adhered onto a glass-bottom dish, precoated with 10 μg/mL mAb HIT3a, and eGFP lifetime before and after acceptor (mCherry) photobleaching was monitored. Shown are pseudocolored eGFP lifetime images, scaled between 1.3 and 2.3 ns. mCherry fluorescence recovery is shown in Fig. S4*F*. *Right:* Corresponding cumulative eGFP lifetime histograms. (Scale bar, 2 μm.) (*D*) Lck-deficient J.CaM1 cells stably expressing the ZIP^{WT} reporter were adhered onto a poly-D-lysine–coated glass-bottom dish for 10 min. eGFP fluorescence lifetime was monitored using TCSPC-FLIM before and 5 min after addition of 1 mM sodium pervanadate. In this Lck-deficient cell line, 5 min stimulation with pervanadate results in a FRET increase at the plasma membrane but not in the intracellular vesicles. (Scale bar, 20 μm.)

membrane. These results further demonstrate that plasma membrane-localized CD3ζ actively exchanges with internalized pool.

Accumulation of tyrosine-phosphorylated CD3ζ on intracellular vesicles suggested that endosomes may contain a tyrosine kinase activity responsible for the phosphorylation of internalized CD3ζ. Indeed, preincubation with PP2 or expression of the reporter in Lck-deficient cell line J.CaM1 attenuated FRET signal from the vesicular compartment (Fig. 3*A*), suggesting that endosomal Lck may play such role. Consistent with previous reports (20, 21), we found that tyrosine kinase Lck is localized both at the plasma membrane and Rab5 and Rab11-positive recycling endosomes (Fig. S4*G*). Immunofluorescent staining with an antibody against phosphotyrosine in the activation loop of Src family kinases (pY418 in Src, pY394 in Lck) demonstrated that in CD3 antibody-stimulated cells, activated tyrosine kinase(s) localized to the plasma membrane and intracellular vesicles, partially colocalizing with internalized reporter (Fig. S4*H*). These results suggest that an active tyrosine kinase on endosomes may contribute to CD3ζ phosphorylation.

Finally, we asked whether endosomal Lck is required for CD3ζ phosphorylation in the intracellular vesicles. Interestingly, in the Lck-deficient J.CaM1 line, 5-min stimulation by pervanadate rapidly increased FRET at the plasma membrane but not on the intracellular vesicles (Fig. 4*D*). This is in contrast to the wild-type E6.1 Jurkat cells, in which pervanadate induced ZIP reporter phosphorylation both at the plasma membrane and on endosomes (Fig. 3*A*). Consistent with its slow internalization kinetics, tyrosine-phosphorylated ZIP^{WT} accumulated in the endosomal compartment some 35 min after stimulation (Fig. S4*I*). These results demonstrate that phosphorylation of endosomal CD3ζ is entirely Lck dependent, whereas the plasma-membrane CD3ζ is phosphorylated by Lck as well as other redundant tyrosine kinases. Given that CD3ζ internalization is relatively slow (Fig. S4 *B* and *C*), rapid pervanadate-induced phosphorylation of the reporter in the wild-type but not Lck-deficient J.CaM1 cells suggests that internalized CD3ζ is a direct substrate of endosomal Lck or Lck-dependent tyrosine kinase. The different patterns of the CD3ζ phosphorylation at the plasma membrane and endosomes in the wild-type and Lck-deficient J.CaM1 cells suggest that intracellular trafficking redistributes CD3ζ into compartments with signaling environment distinct from the plasma membrane.

Discussion

In this study, we have developed unique reporters that allow monitoring of TcR/CD3 phosphorylation in live cells. The proposed strategy offers several advantages over conventional immunofluorescent staining using phospho-specific antibodies: the reporters allow specific monitoring of phosphorylation dynamics in individual cells, are compatible with fixed and live cell imaging, and can be used in combination with other probes or immunofluorescent staining to study the kinase-driven phosphorylation of the TcR/CD3 receptor in vivo.

Using these reporters, we have documented the presence of tyrosine-phosphorylated CD3ζ in the endosomal compartment in unstimulated and activated cells. Activation-dependent down-modulation of TcR/CD3 and other plasma membrane-localized receptors had long been associated with their lysosomal degradation. Indeed, in agreement with previous reporters (2, 10, 18), we also observed increased activation-dependent colocalization of internalized CD3ζ with lysosomes. However, a significant subpopulation of intracellular CD3ζ was retained in the endosomal vesicles that are clearly distinct from lysosomes. Interestingly, we found that internalized CD3ζ was heavily tyrosine phosphorylated, indeed more strongly so than at the plasma membrane, both in activated and a subpopulation of unstimu-

lated cells. A similar pattern of tyrosine phosphorylation was observed in activated T cells previously (22), although the generic antiphosphotyrosine antibody used in the study did not allow identification of the phosphorylated protein.

The reporters described here also allowed us to examine the source of endosomal tyrosine-phosphorylated CD3ζ. Although some of the internalized phosphorylated CD3ζ may derive from internalization of the plasma membrane material, internalized CD3ζ could be a direct substrate of kinase-active Lck present on Rab11-positive endosomes. Indeed, dynamics of the ZIP reporter phosphorylation in Lck-deficient J.CaM1 cells demonstrates that although Lck is dispensable for CD3ζ phosphorylation at the plasma membrane, it is required for local phosphorylation of the ζ subunit on endocytic vesicles.

The presence of tyrosine-phosphorylated CD3ζ on endosomes raises the possibility that TcR/CD3-proximal signaling may continue to propagate after receptor internalization from the plasma membrane. Although active signaling from within endosomes has been reported for a selected group of membrane receptors (reviewed in refs. 23–25), here we directly demonstrate that internalized CD3ζ is signaling competent. The important, albeit nontrivial, questions that remain to be answered are whether distinct TcR/CD3-dependent signaling pathways can be traced specifically to the plasma-membrane and intracellular pools of CD3ζ and how these pathways depend on TcR/CD3 trafficking within the cell. The reporters described here provide tools for addressing these and other questions on the dynamics of TcR/CD3 signaling.

Materials and Methods

Microscopy. Confocal and FLIM images were collected using a Zeiss LSM510 NLO laser scanning system (Carl Zeiss MicroImaging) mounted on an Axiovert 200M inverted microscope equipped with a single-channel SPC-830 TCSPC imaging module (Becker-Hickl). The images were acquired using Plan-Apochromat 63×/1.4 or 100×/1.4 oil immersion objectives.

For spatially resolved time-correlated single-photon counting (TCSPC-FLIM), eGFP fluorescence was excited at 1–4 μW, 476 nm generated by frequency doubling of 952 nm line from a Ti:Sapphire Mai-Tai HP laser (Spectra-Physics) at 80.04 MHz repetition rate. eGFP emission after 525/50 bandpass filter (Chroma Technology) was detected using a PMC-100 photomultiplier (Becker-Hickl) mounted to the fiber-out port of the confocal scanhead. Approximately 10^2 to 10^3 photons per pixel were collected for 256 × 256 image over 1–3 min exposure.

Image Acquisition and Analysis. Confocal images were acquired using LSM510 software v. 4.0 SP2 (Carl Zeiss MicroImaging). FLIM images were acquired using SPC v. 8.72 software; eGFP lifetime images and cumulative lifetime histograms were generated using SPCImage v.2.9.10 software. PDM (product of differences of the mean) images, overlap coefficient *R*, and Mander's coefficient R_r were calculated using intensity correlation analysis plugin (as described in ref. 26) for ImageJ. Details of acquisition conditions and image analysis are summarized in Table S1. Apparent FRET efficiency was calculated as $E = 1 - \tau_{DA}/\tau_D$, where τ_D and τ_{DA} are the apparent eGFP fluorescent lifetime in the absence or presence of the acceptor, respectively. Apparent sensitized emission I_s was calculated for each background-corrected frame as $I_s = I_{DA} - B \cdot I_D - C \cdot I_A$, where I_{DA} is acceptor emission upon donor excitation, I_D is donor emission upon donor excitation, and I_A is acceptor emission upon acceptor excitation. Scalar donor bleed-through (*B*) and direct acceptor excitation (*C*) factors were estimated from cells expressing CD3ζ-eGFP or mCherry-tSH2$^{ZAP\text{-}70}$ only using instrument settings identical to those for measuring sensitized emission.

ACKNOWLEDGMENTS. We thank Holly Aaron for assistance with TCSPC-FLIM and John R. James, Art Weiss, and Mark von Zastrow for critical reading of the manuscript. I.A.Y. is the Genentech fellow of the Jane Coffin Childs Memorial Fund for Medical Research. This investigation has been aided by a grant from the Jane Coffin Childs Memorial Fund for Medical Research.

1. Underhill DM, Goodridge HS (2007) The many faces of ITAMs. *Trends Immunol* 28: 66–73.
2. Valitutti S, Müller S, Salio M, Lanzavecchia A (1997) Degradation of T cell receptor (TCR)-CD3-zeta complexes after antigenic stimulation. *J Exp Med* 185:1859–1864.
3. von Essen M, et al. (2004) Constitutive and ligand-induced TCR degradation. *J Immunol* 173:384–393.
4. Lillemeier BF, et al. (2010) TCR and Lat are expressed on separate protein islands on T cell membranes and concatenate during activation. *Nat Immunol* 11:90–96.
5. Yokosuka T, et al. (2005) Newly generated T cell receptor microclusters initiate and sustain T cell activation by recruitment of Zap70 and SLP-76. *Nat Immunol* 6:1253–1262.
6. Geisler C (2004) TCR trafficking in resting and stimulated T cells. *Crit Rev Immunol* 24: 67–86.
7. Isakov N, et al. (1995) ZAP-70 binding specificity to T cell receptor tyrosine-based activation motifs: the tandem SH2 domains of ZAP-70 bind distinct tyrosine-based activation motifs with varying affinity. *J Exp Med* 181:375–380.
8. Dietrich J, et al. (1999) TCRzeta is transported to and retained in the Golgi apparatus independently of other TCR chains: implications for TCR assembly. *Eur J Immunol* 29: 1719–1728.
9. Labadia ME, et al. (1997) Interaction between the SH2 domains of ZAP-70 and the tyrosine-based activation motif 1 sequence of the zeta subunit of the T-cell receptor. *Arch Biochem Biophys* 342:117–125.
10. Methi T, Berge T, Torgersen KM, Taskén K (2008) Reduced Cbl phosphorylation and degradation of the zeta-chain of the T-cell receptor/CD3 complex in T cells with low Lck levels. *Eur J Immunol* 38:2557–2563.
11. Straus DB, Weiss A (1992) Genetic evidence for the involvement of the lck tyrosine kinase in signal transduction through the T cell antigen receptor. *Cell* 70:585–593.
12. Qian D, Mollenauer MN, Weiss A (1996) Dominant-negative zeta-associated protein 70 inhibits T cell antigen receptor signaling. *J Exp Med* 183:611–620.
13. Douglass AD, Vale RD (2005) Single-molecule microscopy reveals plasma membrane microdomains created by protein-protein networks that exclude or trap signaling molecules in T cells. *Cell* 121:937–950.
14. Varma R, Campi G, Yokosuka T, Saito T, Dustin ML (2006) T cell receptor-proximal signals are sustained in peripheral microclusters and terminated in the central supramolecular activation cluster. *Immunity* 25:117–127.
15. Carrasco YR, Navarro MN, Toribio ML (2003) A role for the cytoplasmic tail of the pre-T cell receptor (TCR) alpha chain in promoting constitutive internalization and degradation of the pre-TCR. *J Biol Chem* 278:14507–14513.
16. D'Oro U, et al. (2002) Regulation of constitutive TCR internalization by the zeta-chain. *J Immunol* 169:6269–6278.
17. Das V, et al. (2004) Activation-induced polarized recycling targets T cell antigen receptors to the immunological synapse; involvement of SNARE complexes. *Immunity* 20:577–588.
18. Ouchida R, et al. (2008) A lysosomal protein negatively regulates surface T cell antigen receptor expression by promoting CD3zeta-chain degradation. *Immunity* 29: 33–43.
19. D'Oro U, Vacchio MS, Weissman AM, Ashwell JD (1997) Activation of the Lck tyrosine kinase targets cell surface T cell antigen receptors for lysosomal degradation. *Immunity* 7:619–628.
20. Gorska MM, Liang Q, Karim Z, Alam R (2009) Uncoordinated 119 protein controls trafficking of Lck via the Rab11 endosome and is critical for immunological synapse formation. *J Immunol* 183:1675–1684.
21. Luton F, Legendre V, Gorvel JP, Schmitt-Verhulst AM, Boyer C (1997) Tyrosine and serine protein kinase activities associated with ligand-induced internalized TCR/CD3 complexes. *J Immunol* 158:3140–3147.
22. Ley SC, Marsh M, Bebbington CR, Proudfoot K, Jordan P (1994) Distinct intracellular localization of Lck and Fyn protein tyrosine kinases in human T lymphocytes. *J Cell Biol* 125:639–649.
23. Murphy JE, Padilla BE, Hasdemir B, Cottrell GS, Bunnett NW (2009) Endosomes: A legitimate platform for the signaling train. *Proc Natl Acad Sci USA* 106:17615–17622.
24. Sadowski L, Pilecka I, Miaczynska M (2009) Signaling from endosomes: Location makes a difference. *Exp Cell Res* 315:1601–1609.
25. von Zastrow M, Sorkin A (2007) Signaling on the endocytic pathway. *Curr Opin Cell Biol* 19:436–445.
26. Li Q, et al. (2004) A syntaxin 1, Galpha(o), and N-type calcium channel complex at a presynaptic nerve terminal: Analysis by quantitative immunocolocalization. *J Neurosci* 24:4070–4081.